Nanoscale

Accepted Manuscript

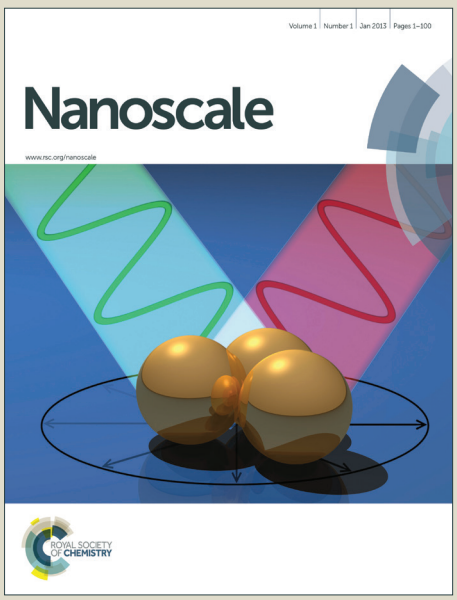

ROYAL SOCIETY OF CHEMISTRY

www.rsc.org/nanoscale

Journal Name

RSCPublishing

ARTICLE

Thick Solid Electrolyte Interphase Grown on Silicon Nancones Anodes during Slow Cycling and Their Negative Effects on Performance for Li-ion Batteries

Cite this: DOI: 10.1039/xoxxoooooox

Received ooth January 2012,
Accepted ooth January 2012

DOI: 10.1039/xoxxoooooox

www.rsc.org/

Fei Luo, [a] Geng Chu, [a] Xiaoxiang Xia, [a] Bonan Liu, [a] Jieyun Zheng, [a] Junjie Li, *[a] Hong Li, *[a] Changzhi Gu[a] and Liquan Chen [a]

Thickness, homogeneity and coverage of the surface passivation layer on Si anode for Li-ion batteries have decisive influences on the cyclic performance and coulombic efficiency, but related information is difficult to obtain, especially during cycling. In this work, a well-defined silicon nanocones (SNCs) on silicon wafer sample has been fabricated as a model electrode in lithium ion batteries for investigating the growth of the surface species on the SiNCs electrode during cycling using *ex situ* scanning electronic microscopy. It is observed that an extra 5 μm thick layer is covered on the top of the SNCs after 25 cycles at 0.1C. This top layer has proved as a solid electrolyte interphase (SEI) layer by designing an solid lithium battery. It is noticed that the SEI layer is much thinner at a high rate of 1C. The cyclic performance of SiNCs at 1C looks much better than the same electrode at 0.1C in the half cell. Our finding demonstrates clearly that the formation of the thick SEI on the nanostructured naked Si anode during low rate cycling is a serious problem for practical application. The in depth understanding of this problem may provide valuable guidance in designing Si based anode materials.

Introduction

In order to satisfy increasing demanding on high energy density Li-ion batteries for various applications, high capacity alloy-type materials containing Sn,[1, 2] Ge,[3-5] Ga[6, 7] and Si[8-10] have been investigated widely for replacing graphite anode. Among all candidates,[11, 12] silicon-based materials are the most promising materials due to the highest theoretical capacity of 3580 mAh/g for forming $Li_{15}Si_4$,[13, 14] abundant sources, environmentally benign and low cost. After comprehensive studies, [12, 15-17] two problems become the major challenges for practical application. Firstly, the insertion of lithium will cause the expansion of Si clusters/grains/particles unavoidably. The volume variation of Si particles during lithiation and delithiation is proportional to the Li-storage capacity linearly and could reach to 320% for fully lithiation.[18] Such a conclusion is applicable to both crystalline and amorphous silicon. Drastic volume variation could lead to the cracking of the large particles (>300 nm), peeling off of active material layer from the current collector, losing electronic contact, exposing of fresh surface in the electrolyte, destroying the surface passivation films. In addition, most of devices cannot allow significant expansion (< 5-20%) of the battery inside. Consequently, designing of the Si-based electrode in Li-ion batteries has to consider this practical requirement and limits the total capacity or total volume variation of the electrode to an acceptable level.

Secondly, it has been found that the solid electrolyte interphase (SEI) layer on silicon anode is very thick, inhomogeneous and not stable during electrochemical cycling.[19, 20] The thickness of SEI layer at the surface of silicon can be more than 800 nm (based on SEM image).[21, 22] It is also noticed that the coverage of the SEI film could be as low as 60% after the first cycle.[20] Consequently, the initial coulombic efficiency is lower than 90%. The coulombic efficiency reaches above 99% after several cycles but cannot approach above 99.8% in successive cycles. This is more apparently for high surface area Si-based anodes. It has been found that Si-based anodes can show much better cyclic performance in the half lithium cell than that in the full cell. In full Li-ion batteries, cathode acts as lithium source. Low coulombic efficiencies mean irreversible capacity loss. Therefore, lithium from cathode will be consumed irreversibly and leads to fast capacity fading in the full battery. In addition, the formation of thick SEI means the consumption of the electrolyte and the increase of the internal resistance. Such situation is not significant in the electrolyte flooded half cell due to excess lithium source and enough electrolyte.

In view of fundamental research, it is necessary to understand the growth and coverage of the SEI on Si anode during the cycling. However, direct experimental investigation has rarely been reported

due to irregular and varied morphology for most of Si-based anode materials.

Herein, a ICP cryogenic silicon etching method is developed to fabricate well-defined SNCs arrays with high aspect ratio on the full silicon wafer. This nanocone structure has several advantages for investigating the SEI film. Firstly, the SNCs are free of conductive additive and binders, eliminating the influence of conductive additives and binders on the growth of SEI on silicon anode. Secondly, the uniqueness of high aspect ratio of SNCs can offer free space to accommodate the volume change for maintaining stable structure during electrochemical cycling. Thirdly, the SEM characterization for silicon nano-particles (or amorphous Si thin films) is complicated by the fact that it is difficult to visually distinguish the SEI from the silicon region. The SNCs have the characteristic of regular appearance, which is favorable for the SEM observation.

Experimental

Materials

All reagents and solvents were used as received. Ethylene carbonate (EC, ≥99%),dimethyl carbonate (DMC, ≥99%), lithium hexafluorophosphate ($LiPF_6$, ≥99.99%) were purchased from Alfa Aesar. Silicon wafer (4 inches, p(100)) was purchased from Beijing Zhongjinkeyi Technology Co., Ltd.

SNCs preparation

SNCs were prepared through etching process, carried out using cryogenic inductively coupled plasma (ICP) reaction ion etching, in which SF_6 and O_2 were served as etching gas at low temperature (-120°C). The formation of silicon nanocone arrays needs firstly an anisotropic etching process, which is based on competing etching and passivation process.Adequate balance between etching and passivation results in structures with perfectly vertical sidewall, while excessive passivation results in incomplete removal of passivation layer from the etched field and inflicts micro masking, which play a key role in further formation of silicon nanocone structure.[23, 24] As the etching proceeds, a random array of SNCs will form. In the etching process, the height, the width, sloping angle and density of SNCs could be tuned by selecting suitable plasma etching condition, such as process pressure, platen power, flow ration (SF_6/O_2) and temperature. SNCs before cycling were cut into electrodes with the size of 0.5cm*0.5cm and vacuum dried for more than 5h at 120 °C to remove moisture from the electrode.

Electrochemical testing

Swageloke-type two-electrode batteries were assembled in an Ar-filled glove box (MBraun, H_2O and O_2 < 0.1 ppm). SNCs were used as working electrode, and lithium foil as counter electrode. The electrolyte was 1 mol•L^{-1} $LiPF_6$ dissolved in ethylene carbonate (EC): dimethyl carbonate (DMC) (1:1, v/v). Electrochemical cycling of assembled half-batteries was performed by a Land BA2100A battery tester (Wuhan, China). All batteries were galvanostatically discharged (lithiated) to limited capacity (100 μAh cm^{-2}) and charged (delithiated) to 2.0 V vs. Li^+/Li at room temperature. The current density of 0.1C, 0.5C and 1C is 10 μA cm^{-2}, 50 μA cm^{-2} and 100 μA cm^{-2}, respectively.

Assembling of a Solid state battery (SSB)

The SSB was assembled in an full of Ar-filled glove box by the following steps: (1) the cell after the 25th cycle at 0.1C was disassembled, separator between the SNCs and lithium foil was removed (2) The SNCs was washed by anhydrous DMC for several times to make sure no residual of $LiPF_6$. The SNCs was vacuum dried for more than 5h to make sure no residual of solvent (3) The SNCs after above treating process was used as working electrode , lithium foil was as counter electrode. In this battery, 5 μm SEI layer on the SNCs acted as the solid electrolyte.

Characterization

The batteries after the 1st, 2nd, 10th, 15th, 20th and 25th cycle at 0.1C were disassembled in Ar-filled glove box and the SNCs were washed by anhydrous DMC for several times to make sure no residual of $LiPF_6$, and then the samples were vacuum dried for more than 5h to remove solvent. The morphologies of SEI at the surface of SNCs were observed by a Hitachi S-4800 scanning electron microscope (SEM) equipped with energy dispersive X-ray spectroscopy (EDS). The samples were sealed in a special vacuum transfer box during the sample transfer from the glove box to the SEM chamber.

Results and discussion

The aspect ratio of as-fabricated SNCs is controlled by tuning the etching pressure as shown in Fig. 1a. The sample with the highest aspect ratio of 10 is chosen in this work due to its large space to alleviate volume variation and avoid cracking [25, 26] as well as possessing space for filling the SEI species. The half-width of each nanocone in the selected SNCs sample is about 200 nm and the height of Si nanocone layer is about 2.02 μm. The first discharge (delithiation) capacity of the SNCs at 0.1C can reaches 83.5 μAh cm^{-2} (corresponding to a specific capacity of 1668 mAh/g, $Li_{1.75}Si$, this is a rough estimation). The coulombic efficiency in the initial cycle is 83.5% and increases to ca. 95% in the subsequent cycles. Fig. 1c exhibits the cycle performance of SNCs at 0.1C.

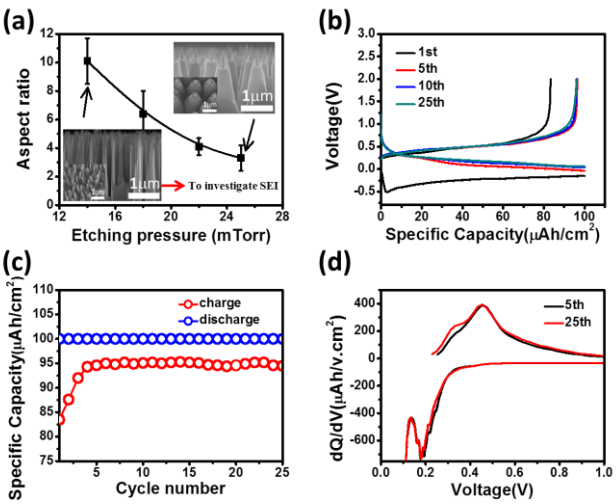

Fig.1. (a) Aspect ratio of as-fabricated SNCs on the process pressure, the inserted SEM images represent the highest (left bottom) and the lowest (top right corner) aspect ratio of SNCs in this work. (b) Voltage vs. capacity profile of the SNCs at 0.1C from 1st to 25th cycle (c) The galvanostatic cycling performance of SNCs (current density is 10 μA/cm^2, discharge to the limited capacity at 100 μAh/cm^2) (d) Curves of d Q/d V for the SNCs electrode after the 5th and 25th cycle.

During the first five cycles, the charge (delithiation) capacity increase gradually from 83.5 μAh cm^{-2} to 94.5 μAh cm^{-2} for the first five cycles), indicating an activation process. In this work, the

silicon nanocone electrode was prepared from silicon wafer (4 inches, p(100)) through etching process. Si wafer (460 μm) acts as the substrate layer and the surface silicon nanocone layer has a thickness of 2 μm. Obviously, Si wafer can also take part into the electrochemical reaction. The kinetics for initial lithiaiton is difficult since both Si wafer and silicon nanocones have low electronic conductivity and occur a crystal-to-amorphous phase transition reaction.[27, 28] This is shown clearly in the differential capacity curves (Fig. 1d). One broad Li insertion (alloying) peak at 0.19 V and a peak below 0.19 V and two Li extraction (de-alloying) peaks at 0.32 V and 0.48 V can be seen. Appearance of two peaks in the dQ/dV curves is quite common in the Si-based anodes and can be explained by a two-step amorphous phase transition mechanism, as reported previously.[27, 28] The similarity of the 5th and 25th differential capacity curves indicates that the electrochemical behaviors of SNCs are similar at the 5th and 25th cycle.

It can be seen from Fig.2B that the activity of Si wafer and Si nanocones increase gradually upon cycling due to the increase of the electronic conductivity of lithiated Si and structure variation.

The morphology of the SNCs anodes at different cycles has been investigated by SEM technique. A special sample transfer holder was used for the Hitachi 4800 microscope in order to transfer the lithiated samples from the glove box to the SEM vacuum chamber without exposure to air. After the first cycle, the morphology variation of the SNCs electrode is not obvious (Fig. 2a) compared to the original sample (see Fig. 1a left inset). EDS analysis indicates that the atomic ratio of Si and O is 96.08 and 3.92%, respectively, without the presence of F and C. As we reported recently, the SEI may not cover the whole surface of Si thin film electrode.[20] The absence of C and F means that the content of the SEI is very low and cannot be detected by the EDS. This can be understood. Actually, the Si nanocone electrode has low electronic conductivity. As shown in the first discharge curve (Fig.1b), the lithiation voltage is less than 0.0 V due to very high initial polarization. In this experimental, the discharge was performed by controlling constant capacity. Therefore, lithiation is kinetically difficult, but still occurs after the voltage drops down below to 0.0 V. After the first discharge, the Si nanocone electrode is activated and lithiated Si should have enhanced activity and electronic conductivity. Therefore, after the first cycle, the electrochemical behaviour of Si nanocone electrode becomes normal. The first cycle can be understood as an activation process although the detailed mechanism is still very clear.

After the second cycle, some granular particles are found on the SNCs (Fig. 2b). Top view shown in Fig. 2b inset indicates that the electrode is well preserved. EDS analysis indicates the presence of Si, O, F, and C (89.76, 2.52, 2.0 and 5.72%, respectively), consistent with the deposition of the SEI. After the 10th cycle, the amount of granular SEI particles increases significantly and can be seen even on the top of the electrode (Fig. 2c inset). EDS analysis of electrode reveals that concentrations of O, F, C, and P (3.59, 6.22, 3.94, and 0.23%, respectively) increases significantly, indicating the increase of the SEI species. After the 15th cycle, the film-like species become more significant and the cavities between each individual Si nanocone decreases obviously compared to Fig. 2a. The atomic ratio of O, C, F, P increases to 9.56%, 25.89%, 11.79% and 0.63% respectively.

After 20 cycles, no cavity can be seen from top and the surface is covered completely. The atomic ratio of O, C, F, P increases to 18.05%, 17.94%, 20.85 and 1.47% respectively. After the 25th cycle, some cracks can be seen from top and the area without crack seems quite flat. The atomic ratio of O, C, F, P increases to 42.43%, 25.97%, 23.63% and 1.76 % respectively.

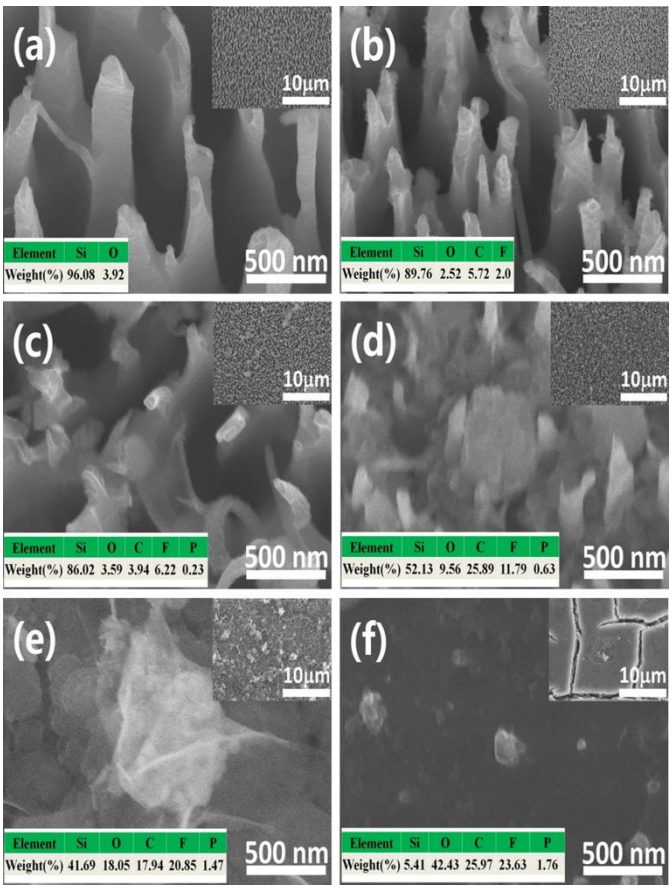

Fig.2. SNCs SEM images for (a) 1st cycle (b) 2nd cycle (c) 10th cycle (d) 15th cycle (e) 20th cycle (f) 25th cycle. The left bottom inset of each SEM image is for the elemental concentrations of the SNCs, as determined by EDS. The top right corner inset of each SEM image is surface morphology at low magnification.

The growth of the SEI species and the filling of the SEI species into the cavities between each Si nanocone can be seen clearly from the side view shown in Fig. 3. After 20 cycles, all cavities have been filled by the SEI species and the top layer becomes flat. Another extra layer is covered on the surface of the Si nanocone array electrode after 25th cycle.

Zoomed cross-section image of the sample after 25th cycle and the corresponding EDS mapping is shown in Fig. 4. Based on the cross section SEM images and EDS mapping of the SNCs after 25 cycles as shown above, the mean thickness from the bottom of SNCs to the top of SEI is 7.1 μm. The height of SNCs layer is about 2.02 μm. Thus, the distance between the top of nancones and the top of SEI layer is not 5.08 μm,very close to 5μm. the top layer has a thickness of 5 μm and composed of F, O, C, P and negligible Si. Therefore, it can be claimed undoubtedly that the top layer should be a SEI layer, which will be confirmed further in later section by testing in a solid battery.

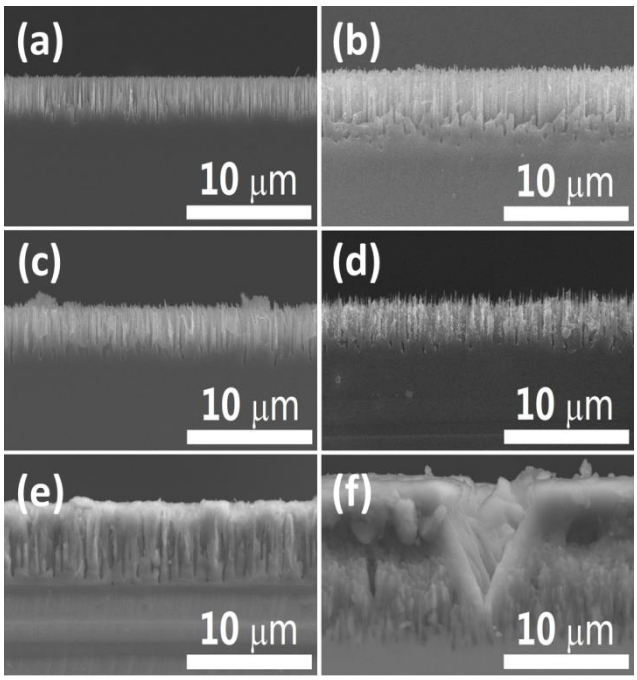

Fig.3. Cross section SEM images of the SNCs for: (a) primary sample (b) 5th cycle (c) 10th cycle (d) 15th cycle (e) 20th cycle (f) 25th cycle.

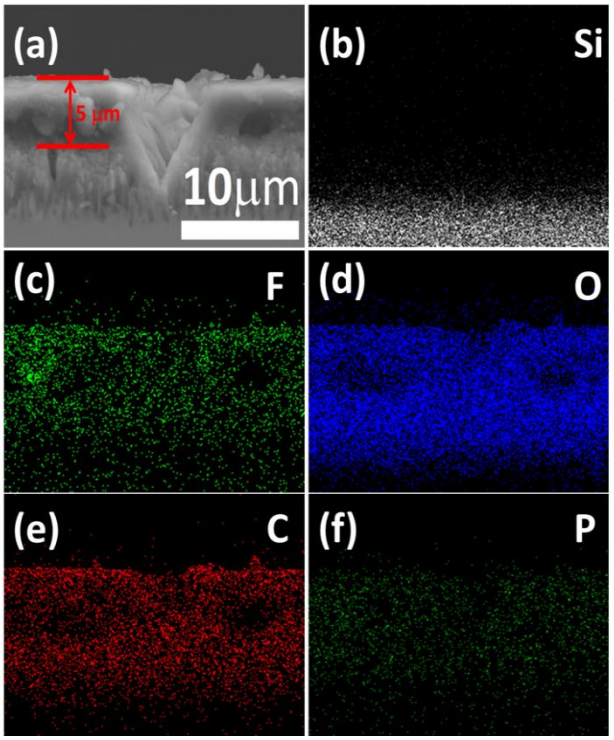

Fig.4. Elemental mapping image of cross section for SNCs after the 25th cycle.

According to Fig. 2-Fig. 4, a scheme with inset SEI images of the side-view at different cycles is shown in Fig. 5. The SEI growth on the SNCs electrode includes five steps as follows:

1) Nucleation of some granular SEI particles on the surface of the SNCs at the first two cycles (Fig. 5b).
2) Aggregation of granular SEI particles after the 10th cycle (Fig. 5c).
3) Filling of cavities between SNCs after the 15th cycle (Fig. 5d).
4) Further growth of the SEI and the formation of an extra top layer after the 20th cycle (Fig. 5e).
5) Growth to a 5 μm extra top layer
6) The cracking of the SEI layer is also seen after the 25th cycle (Fig. 5f).

Above results indicate two points:

1) Complete coverage of the SEI layer on such nanostructured Si anode needs many cycles.
2) Thickness of the SEI layer can reach to 5 μm.

Our recent force-curve investigation on the coverage of the SEI on Si thin film electrode indicates that the SEI can only cover 60% surface area of a flat Si thin film electrode even after keeping constant potential at 5 mV vs Li^+/Li in a half cell for 48 hours.[20] The incomplete coverage of the SEI layer could be originated from several factors. One is inhomogeneous surface electronic conductivity. Once certain area of Si particles/electrode is inserted by lithium, local electronic conductivity increases sharply. This area could become more active for both lithium insertion and electrochemical reduction of the electrolyte compared to unreacted Si areas. In addition, the growth of the SEI on anode is a dynamic competition process among the nucleation of the SEI species, dissolution of the SEI species and deposition on existed SEI layer or on naked area. If the surface is inhomogeneous, then nucleation and growth of the SEI is inhomogeneous.[20]

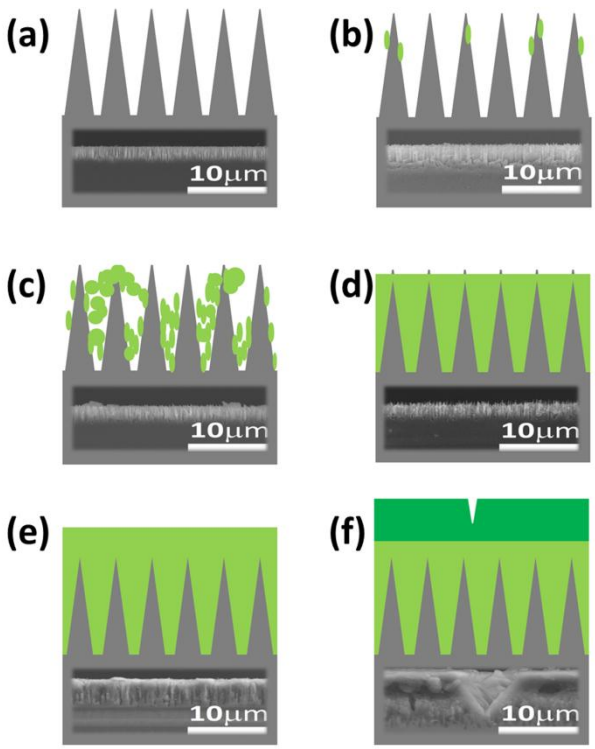

Fig.5. The scheme of the procedures for forming SEI on SNCs electrode .The insets are the cross section for SNCs SEM images for (a) primary sample (b) 2nd cycle (c) 10th cycle (d) 15th cycle (e) 20th cycle (f) 25th cycle.

It is observed that the extra SEI top layer is as thick as 5 μm. It is well accepted previously that the thickness of the SEI should be closed to the electron tunneling length. The effectiveness of this conclusion needs four presumptions:

1) SEI is dense;
2) Growth of the SEI is homogeneous,
3) SEI is stable after growth;
4) SEI is electronic insulating.

Our recent investigations deny the first three presumptions.[20] The last one is still not clear since the direct measurement on the electronic conductivity of the SEI seems difficult (A conductive AFM or STM mapping may clarify this issue, we plan to do it in near future). Thickness of the SEI above the electronic tunneling path have also been observed in other anode materials.[21, 22, 29, 30] In addition, the charge capacities still remain much lower than the discharge capacity even after 25 cycles, with the Coulombic efficiency is around 95%. It means that the SEI layer could grow further even after 25 cycles unless that the liquid electrolyte is exhausted or the SEI layer becomes enough compact when all the nanopores in SEI is filled up completely. In real Li-ion batteries, it is known that the SEI grows continuously even after 1000 cycles for graphite anode. In many cases, the Li-ion batteries are failed due to the exhaustion of the electrolyte for forming the SEI. A good material design should consider adding effective SEI controlling additive or coating the anode to slow down this side reaction during cycling.

Many reports in literatures claim that nanosized or nanostructured Si anodes show excellent cyclic performance and rate performance, especially at high rate. It is interesting and valuable to investigate the growth of the SEI at high rate since it is convenient for our sample with unique well-defined morphology .

Fig. 6a-d shows clearly that the thick SEI film is not observed after 25 cycles both at 0.5C and 1C. Morphology of the SNCs electrode at 0.5 C and 1C after 25th cycles is closed to that at 0.1C after the 10th cycle and after the 2rd cycle respectively. EDS analysis of the SNCs at 0.5 C and 1C is listed in Table 1 will give the similar results. This suggests clearly that the higher the rate, the thinner the SEI after the same cycle.

The influence of the rate on the thickness of the SEI is not very clear. There could be three possible reasons:

1) **Reaction path,** it has been reported that the reduction of the organic solvents could be either single-electron reaction at low current density or double-electron reaction at high current density.[30, 31] The former tends to form loose alkyl carbonate, the later tends to form dense Li_2CO_3. Such mechanism has been studied well by Aurbach et al previously.[31-32]
2) **Kinetics**, the kinetics of the decomposition of the electrolyte is influenced by the current density. In this experimental, the capacity is fixed. Lithiation and the formation of the SEI are two parallel reactions during discharging. At high rate, the formation of the SEI may not follow up.
3) **Chemical reaction,** lithiated Si could react with solvents and salts chemically. This is known from the NMR results done by Grey et al.[33] At high rate, the discharge period is much short than that at low rate. Therefore, the period for chemical side reaction is much different. This will happen if the SEI is porous.

Up to now, there are no direct quantitative experimental evidence to disclose the relationship between the SEI thickness and the rate. And it is not clear which factor plays the main role. It needs further clarification in future.

Table 1. EDS element mapping results of the SNC electrode at different states .

State	Si	O	C	F	P
0.1C,1st	96.08%	3.92%	/	/	/
0.1C,2nd	89.76%	2.52%	5.76%	2.0%	/
0.1C,10th	86.02%	3.59%	6.22%	3.94%	0.23%
0.1C,15th	52.13%	9.56%	25.89%	11.79%	0.63%
0.1C,20th	41.69%	18.05%	17.94%	20.85%	1.47%
0.1C,25th	5.41%	42.43%	25.97%	23.63%	1.76%
0.5C,25th	74.54%	6.9%	8.37%	9.38%	0.81%
1C,25th	87.9%	0.8%	5.9%	5.4%	/

Fig. 6e shows that the SNCs can achieve better cyclic performance at 1C compared to 0.5C and much better than that obtained at 0.1C, under condition of same limited discharge capacity (100 μAhcm^{-2}). The reversible capacity after 300 cycles at 1C remains 97.3 μAhcm^{-2}, much higher than 93μAhcm^{-2} tested at 0.5C, not mentioned very poor cyclic performance at 0.1C. Remarkably, it should be mentioned that the average coulomb efficiency during the first 25 cycles at 0.5 C and 1C are 97.6% and 98.9% respectively, both are much higher than 95% at 0.1C. Above results confirm that the SNCs can achieve superior cyclic performance and high coulombic efficiency at high rate. However, the same electrode shows poor performances at low rate due to continuous growth of the very thick SEI layer.

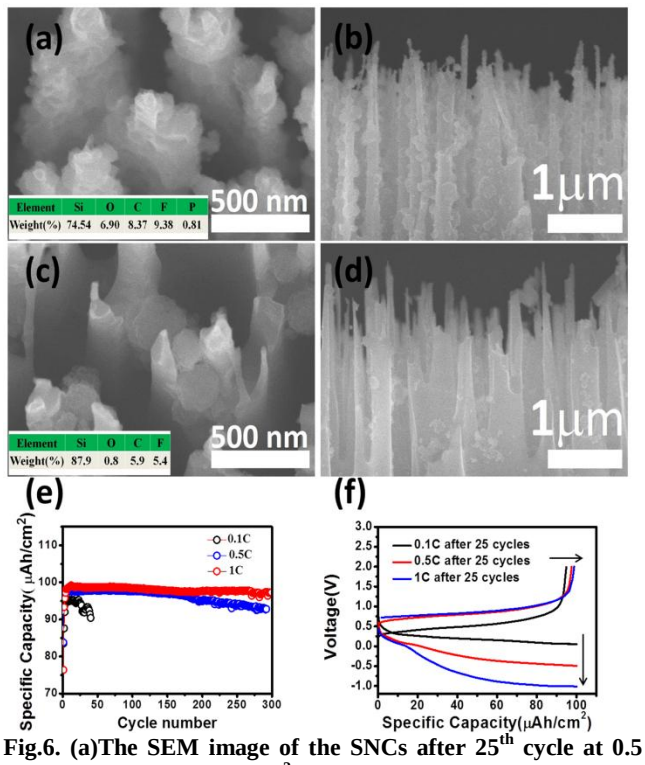

Fig.6. (a)The SEM image of the SNCs after 25th cycle at 0.5 C (current density 50 μA /cm^2, discharge to the limited capacity at 100 μAh /cm^2) (b) The cross section SEM image of the SNCs after 25th cycle at 0.5 C (c) The SEM image of the SNCs after 25th cycle at 1C (current density 100 μA /cm^2) (d) The cross

section SEM image of the SNCs after 25th cycle at 1C (e) the galvanostatic cycling performance of the SNCs at 0.1C, 0.5C and 1C (f) voltage vs. capacity profile of the SNCs electrode after the 25th cycle at 0.1C, 0.5C and 1C.

According to above investigations, the growth of the thick SEI at low rate is significantly. It will consume the lithium from the cathode and the electrolyte in the full Li-ion batteries irreversibly. Therefore, the direct exposure of the Si surface to the electrolyte in nonaqueous Li-ion batteries should be avoided. The surface coating, forming nanocomposite with a protective shell, adding effective additives are recommended for practical design.[34-36]

In above discussion, we presume that the observed extra granular particles and the top coverage layer are the solid electrolyte interphase, however, except for EDS mapping, no direct evidence is provided to confirm that the top layer is the SEI. Actually, the SEI should play the role as solid electrolyte. An experimental was designed to confirm directly that the top layer has the functionality of the SEI. After 25th cycle, the half-cell was dissembled. A new solid cell was fabricated. The "SEI" covered SNCs electrode was used as the cathode and the top "SEI" layer grown on the SNCs electrode acts as the solid electrolyte. A fresh lithium foil was pasted on the top of the "SEI" covered SNCs electrode. Then this Li/SEI/Si solid state battery (SSB) was cycled.

Fig. 7a shows the scheme of the cell and the electrochemical performances. The electrochemical test of this SSB was performed at the rate of 0.1C (0.1C = 10 μAcm^{-2}) at room temperature. As shown in Fig. 7b-c, the first reversible capacity is 31.6 μAh cm^{-2}. This value is 1/3 of the discharge capacity (100 μAh cm^{-2}) using liquid electrolyte. And the reversible capacity increases to 86.2 μAh cm^{-2} in the subsequent cycles. The increase of the capacity should be related to the improvement of the solid/solid interface. The main conclusion from this experimental is that the top "SEI" layer indeed has the functionality of solid electrolyte layer: preventing the electronic conducting but providing lithium ion conducting properties as electrolyte.

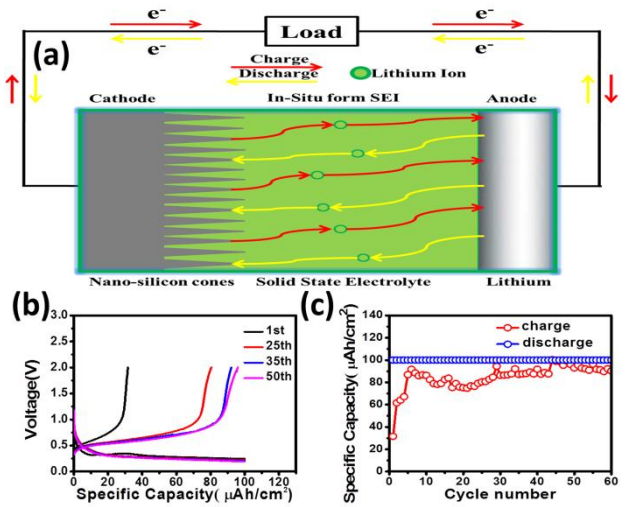

Fig.7. (a) The schematic diagram of a solid state battery using in-situ SEI formed after 25 cycles in a Li/Si nanocone cell as the solid electrolyte (b) voltage vs. capacity profile of SSB at 0.1C from 1st to 50th cycle((current density 10 μAh cm^{-2}, discharge to the limited capacity at 100μAh cm^{-2}) (c) the galvanostatic cycling performance of the SSB.

It has to be mentioned that similar cell could not operate if the top-layer covered SNCs electrode was replaced by the fresh SNCs electrode (Fig. 8a) or could not operate properly when the SNC electrode was cycled only 10 times (Fig. 8b). The above results confirm unambiguously that the top 5μm layer shown in Fig.4a is the solid electrolyte interphase grown gradually on the SNCs electrode during the electrochemical cycling.

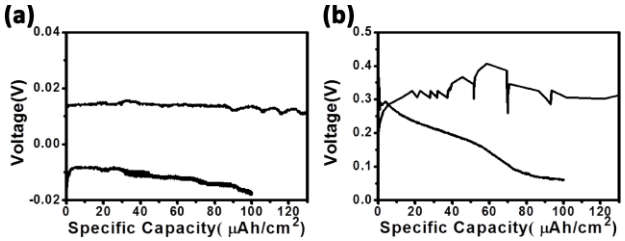

Fig.8. (a) Charge and discharge curves of SSB（solid state battery）using the primary SNCs before cycling, (b) Charge and discharge curves of SSB using the SNCs after 10 cycles.

It is slightly surprised that this layer seems have high ionic conductivity since the prepared cell can operate at 0.1C at room temperature and the polarization is not very high. The detailed chemical composition of this top SEI layer will be clarified in future by other techniques, such as SIMS, XPS and FTIR. It reminds us that this could be a new way to prepare solid electrolyte or a way to introduce artificial solid electrolyte in the composite composite solid lithium ion electrolyte.

Conclusions

SEM investigations on the morphology changes of the well-defined silicon nanocones array electrode in half cells at different cycles at different rates indicate:

(1). Nucleation and growth of the SEI is inhomogeneous and the full coverage of the SEI could be achieved after 10-20 cycles;
(2). The SEI could be as thick as 5 μm when the electrode is discharged at low rate;
(3). The nanostructured Si nanocones electrode could show excellent cyclic performance and high coulombic efficiency at high rate in half cell, but suffers at low rate. It means that such material cannot operate well in the full batteries due to irreversible and significant consumption of lithium from the cathode.
(4). The SEI layer grown during electrochemical reactions could really play the role of the solid electrolyte. It can function well at room temperature. This may inspire us for designing the composite solid electrolytes.

Our finding indicates that direct contact of the Si-based anode material with carbonate electrolyte should be avoided in Li-ion batteries and forming a stable passivation layer on Si-based anode before electrochemical discharging/charging is needed. Further investigations on the microstructure and chemical composition of such thick SEI as well as the growth mechanism and kinetics are carrying out.

Acknowledgements

Financial supports from NSFC project (51325206), "973" project of MOST (2012CB932900), "Strategic Priority Research Program" of the Chinese Academy of Sciences (XDA09010102) and Beijing S&T Project (Z131110000340000) are appreciated.

Notes and references

[a]Beijing National Laboratory for Condensed Matter Physics, Institute of Physics, Chinese Academy of Science, Beijing, 100190, China
e-mail: jjli@iphy.ac.cn, hli@iphy.ac.cn

1. M. Noh, Y. Kwon, H. Lee, J. Cho, Y. Kim and M. G. Kim, *Chem. Mater.*, 2005, **17**, 1926-1929.
2. J. Hassoun, G. Derrien, S. Panero and B. Scrosati, *Adv. Mater.*, 2008, **20**, 3169-3175.
3. C. K. Chan, X. F. Zhang and Y. Cui, *Nano Lett.*, 2008, **8**, 307-309.
4. S. Yoon, C.-M. Park and H.-J. Sohn, *Electrochem. Solid-State Lett.*, 2008, **11**, A42-A45.
5. M. H. Park, Y. Cho, K. Kim, J. Kim, M. Liu and J. Cho, *Angew. Chem.*, 2011, **123**, 9821-9824.
6. R. D. Deshpande, J. Li, Y.-T. Cheng and M. W. Verbrugge, *J. Electrochem. Soc.*, 2011, **158**, A845-A849.
7. W. Liang, L. Hong, H. Yang, F. Fan, Y. Liu, H. Li, J. Li, J. Y. Huang, L.-Q. Chen and T. Zhu, *Nano Lett.*, 2013, **13**, 5212-5217.
8. H. Li, X. Huang, L. Chen, Z. Wu and Y. Liang, *Electrochem. Solid-State Lett.*, 1999, **2**, 547-549.
9. N. Liu, H. Wu, M. T. McDowell, Y. Yao, C. Wang and Y. Cui, *Nano Lett.*, 2012, **12**, 3315-3321.
10. N. Liu, Z. Lu, J. Zhao, M. T. McDowell, H.-W. Lee, W. Zhao and Y. Cui, *Nat.Nanotechnol.*, 2014.
11. U. Kasavajjula, C. Wang and A. J. Appleby, *J. Power Sources*, 2007, **163**, 1003-1039.
12. J. R. Szczech and S. Jin, *Energy & Environmental Science*, 2011, **4**, 56-72.
13. X. H. Liu, H. Zheng, L. Zhong, S. Huang, K. Karki, L. Q. Zhang, Y. Liu, A. Kushima, W. T. Liang and J. W. Wang, *Nano Lett.*, 2011, **11**, 3312-3318.
14. J. Li and J. R. Dahn, *J. Electrochem. Soc.*, 2007, **154**, A156-A161.
15. Y. Yin, L. Wan and Y. Guo, *Chinese Science Bulletin*, 2012, **57**, 4104-4110.
16. M. T. McDowell, S. W. Lee, W. D. Nix and Y. Cui, *Adv Mater*, 2013, **25**, 4966-4984.
17. X. Su, Q. Wu, J. Li, X. Xiao, A. Lott, W. Lu, B. W. Sheldon and J. Wu, *Adv. Energy Mater.*, 2014, **4**.
18. Y. He, X. Yu, Y. Wang, H. Li and X. Huang, *Adv. Mater.*, 2011, **23**, 4938-4941.
19. C. K. Chan, R. Ruffo, S. S. Hong and Y. Cui, *J. Power Sources*, 2009, **189**, 1132-1140.
20. J. Y. Zheng, H. Zheng, R. Wang, L. Ben, W. Lu, L. Chen, L. Chen and H. Li, *Phys. Chem. Chem. Phys.*, 2014, **16**, 13229-13238.
21. P. H. L. Notten, F. Roozeboom, R. A. H. Niessen and L. Baggetto, *Adv Mater*, 2007, **19**, 4564-4567.
22. L. Baggetto, J. F. M. Oudenhoven, T. van Dongen, J. H. Klootwijk, M. Mulder, R. A. H. Niessen, M. H. J. M. de Croon and P. H. L. Notten, *J Power Sources*, 2009, **189**, 402-410.
23. L. Sainiemi, H. Keskinen, M. Aromaa, L. Luosujärvi, K. Grigoras, T. Kotiaho, J. M. Mäkelä and S. Franssila, *Nanotechnology*, 2007, **18**, 505303.
24. H. Jansen, M. De Boer, S. Unnikrishnan, M. Louwerse and M. Elwenspoek, *J. Micromech. Microeng.*, 2009, **19**, 033001.
25. R. Ruffo, S. S. Hong, C. K. Chan, R. A. Huggins and Y. Cui, *J. Phys. Chem. C*, 2009, **113**, 11390-11398.
26. Y. He, X. Yu, Y. Wang, H. Li and X. Huang, *Adv. Mater.*, 2011, **23**, 4938-4941.
27. W. Yanhong, L. Yaoping, Z. Jieyun, Z. Hao, M. Zengxia, D. Xiaolong and L. Hong, *Nanotechnology*, 2013, **24**, 424011.
28. J. W. Wang, Y. He, F. Fan, X. H. Liu, S. Xia, Y. Liu, C. T. Harris, H. Li, J. Y. Huang, S. X. Mao and T. Zhu, *Nano Lett.*, 2013, **13**, 709-715.
29. K. F. Zhong, X. Xia, B. Zhang, H. Li, Z. X. Wang, L. Q. Chen, *J. Power Sources* 2010, **195**, 3300-3308
30. G. Gachot, S. Grugeon, M. Armand, S. Pilard, P. Guenot, J.M. Tarascon, S. Laruelle, *J. Power Sources* 2008, **178**, 409-421.
31. D. Aurbach), B. Markovsky, M.D. Levi, E. Levi, A. Schechter, M. Moshkovich, Y. Cohen, *J. Power Sources* 1999, **81–82** 95-111
32. K. Xu, *Chem. Rev.*, 2004, **104**, 4303–4418.
33. B. Key, R. Bhattacharyya, M. Morcrette, V. Seznec, J. M. Tarascon,C. P. Grey, *J. Am. Chem. Soc.* 2011, **131**, 9239-9249
34. H. Li, Z. Wang, L. Chen, X. Huang, *Adv. Mater.*, 2009, 21, 4593 – 4607.
35. H. Li, J. Hu, X. J. Huang, L. Q. Chen, Chinese patent, ZL 1328805c, 2004.
36. H. Li, X. J. Huang, Chinese patent, ZL 100422112c, 2005.